Mechanism of the Synergistic End-Product Regulation of *Bacillus subtilis* Glutamine Phosphoribosylpyrophosphate Amidotransferase by Nucleotides[†,‡]

Sihong Chen,[§] Diana R. Tomchick,[∥] Dana Wolle,[§] Ping Hu,[⊥] Janet L. Smith,[∥] Robert L. Switzer,[⊥] and Howard Zalkin*[,§]

Departments of Biochemistry and Biological Sciences, Purdue University, West Lafayette, Indiana 47907, and Department of Biochemistry, University of Illinois, Urbana, Illinois 61801

Received May 20, 1997; Revised Manuscript Received July 7, 1997[⊗]

ABSTRACT: *De novo* purine nucleotide synthesis is regulated, at least in part, by end-product inhibition of glutamine PRPP amidotransferase. An important feature of this inhibition is the fact that certain synergistic nucleotide pairs give more than additive inhibition. The physiological importance of synergism is in amplifying regulation by the adenine and guanine nucleotide end products of *de novo* synthesis. Using a new method to quantitate synergism, ADP plus GMP were confirmed [Meyer, E., and Switzer, R. L. (1978) *J. Biol. Chem. 254*, 5397−5402] to give strong synergistic inhibition of *Bacillus subtilis* glutamine PRPP amidotransferase. An X-ray structure of the ternary enzyme·ADP·GMP complex established that ADP binds to the allosteric A site and GMP to the catalytic C site. GMP increased the binding affinity of ADP for the A site by ∼20-fold. Synergism results from a specific nucleotide−nucleotide interaction that is dependent upon a nucleoside diphosphate in the A site and a nucleoside monophosphate in the C site. Furthermore, synergism is enhanced by the competition between nucleotide inhibitor and PRPP substrate for the C site. Purine base specificity results from a backbone carbonyl interaction of $Lys^{305'}$ with the 6-NH_2 group of adenine in the A site and a Ser^{347} Oγ interaction with the 2-NH_2 group of guanine in the C site. Steric considerations favor binding of the nucleoside diphosphate to the A site. Site-directed replacements of key residues increased the nucleotide concentrations needed for 50% inhibition and in some cases perturbed synergism. Mutations in either of the nucleotide sites perturbed function at both sites, supporting the important role of synergism.

Glutamine PRPP[1] amidotransferase catalyzes the initial reaction in *de novo* purine nucleotide synthesis and is the key regulatory enzyme in the pathway. Genes encoding glutamine PRPP amidotransferase have been cloned from more than 20 organisms including bacteria, eukarya, and archea (*1*). However, only the enzymes from *Escherichia coli* (*2*) and *Bacillus subtilis* (*3*) have been purified to homogeneity and are well-characterized. In addition, X-ray structures have been determined for the *E. coli* (*4*, *5*) and *B. subtilis* (*6*) enzymes. These enzymes are both homotetramers. The *E. coli* and *B. subtilis* enzymes are representative of two classes of glutamine PRPP amidotransferase. Enzymes of the *B. subtilis* class are synthesized with an NH_2 terminal propeptide and an Fe−S center, whereas enzymes of the *E. coli* class have neither.

Purine nucleotide biosynthesis is regulated, at least in part, by end-product inhibition by adenine and guanine nucleotides. The patterns for inhibition by adenine and guanine nucleotides differ for the two enzymes. Thus, GMP is the single strongest inhibitor of *E. coli* glutamine PRPP amidotransferase (*2*), and AMP is the strongest inhibitor of the *B. subtilis* enzyme (*7*). Notwithstanding this difference, there is one common distinctive characteristic of the inhibition by nucleotides. Certain pairs of adenine and guanine nucleotides give more than additive inhibition compared to the individual nucleotides, a phenomenon called synergistic inhibition. The strongest synergistic pair for the *B. subtilis* enzyme was reported to be ADP plus GMP (*7*). AMP plus GMP was reported to be a strong synergistic nucleotide pair for the *E. coli* enzyme (*8*), although more recent experiments suggest that GDP plus AMP may be the most effective synergistic pair.[2]

It has been pointed out that synergistic inhibition of glutamine PRPP amidotransferase implies the existence of separate binding sites for adenine and guanine nucleotides on each subunit (*2*, *7*). X-ray structures of the *B. subtilis* (*6*) and *E. coli* (*4*) enzymes have identified four nucleotide sites per half-tetramer, two equivalent allosteric A sites between subunits, each with an adjacent catalytic C site. It has been reported that synergistic binding of GMP to the A site and AMP to the C site could account for the synergistic inhibition of the *E. coli* enzyme (*8*). We report here a more systematic study of the mechanism for synergistic inhibition of the *B. subtilis* glutamine PRPP amidotransferase. The results confirm that ADP and GMP are the most synergistic pair (*7*) and demonstrate that synergistic inhibition results

[†] Supported by United States Public Health Service Grants DK42303 to J.L.S., GM47112 to R.L.S., and GM24658 to H.Z. This is journal paper 15 466 from the Purdue University Agricultural Research Station.

[‡] Atomic models of ADP/GMP-inhibited *Bacillus subtilis* glutamine PRPP amidotransferase and of the free and DON-inactivated *Escherichia coli* enzyme are available from the Protein Data Bank under accession codes 1ao0, 1ECF, and 1ECG, respectively.

* Author to whom correspondence should be addressed.

[§] Department of Biochemistry, Purdue University.

[∥] Department of Biological Sciences, Purdue University.

[⊥] University of Illinois.

[⊗] Abstract published in *Advance ACS Abstracts,* August 15, 1997.

[1] Abbreviations: PRPP, 5-phosphoribosyl-1-pyrophosphate; EGTA, ethylene glycol *bis*(β-aminoethyl ether)-*N,N,N′,N′*-tetraacetate.

[2] J. H. Kim and H. Zalkin, unpublished data.

S0006-2960(97)01189-6 CCC: $14.00

from synergistic binding. An X-ray structure of a ternary enzyme·ADP·GMP complex establishes that ADP binds to the A site and GMP to the C site and that synergism results from a specific interaction between the β-phosphate of a nucleoside diphosphate in the A site and a nucleoside monophosphate in the C site. These results establish the mechanistic basis for synergism.

EXPERIMENTAL PROCEDURES

Plasmids. Plasmid pGZ1 was used for production of the wild type enzyme. Plasmid pGZ1 contains a 1.6 kb *Eco*RI-*Hind*III *purF*$^+$ fragment (*9*) inserted into the corresponding sites of pUC18. For construction of mutants, the *Eco*RI-*Hind*III *purF*$^+$ DNA was transferred to pUC118 to yield pBsF. Mutations were constructed by the method of Kunkel *et al*. (*10*) using pBsF phagemid DNA. The resulting plasmids were named pBsF/S283A, pBsF/K305Q, pBsF/R307Q, and pBsF/S347A.

Overexpression and Enzyme Purification. E. coli strain TX158 (*purF*) (*11*) bearing the wild type or *purF* mutant plasmid was grown in minimal medium (*12*) plus 140 μg/mL ampicillin at 37 °C for 20 h. Cells were harvested and stored in liquid nitrogen. For a typical purification, we used 10 g of cells obtained from 4 L of medium.

For enzyme purification, all buffers were sparged with nitrogen gas prior to use in order to minimize oxidation of the enzyme's Fe−S cluster. All steps were carried out at 4 °C. Cells resuspended in 4 mL of buffer A per gram [50 mM Tris-HCl (pH 8.0), 10 mM $MgCl_2$, 0.1 mM EDTA, 5 mM DTT, and 2 mM AMP] containing 1 mM PMSF were disrupted by two passes through a French Press. Cell extract was obtained by centrifugation for 1 h at 27 000*g*. Protamine sulfate (5 mg per gram of cells) was added to the extract to precipitate DNA. After centrifugation at 27 000*g* for 30 min, the supernatant was applied to a 1.9 × 20 cm column of DEAE-Sepharose equilibrated with buffer A. The column was washed with 300 mL of buffer A and 300 mL of buffer A plus 0.1 M KCl and eluted with a linear salt gradient of 600 mL from 0.1 to 1.0 M KCl in buffer A. Brown-colored fractions containing the enzyme were precipitated by addition of ammonium sulfate to 40% saturation. After centrifugation, enzyme in the brown pellet was recovered by extraction twice with 30% saturated ammonium sulfate. A small colorless pellet that remained was discarded, and the dark brown enzyme solution in buffer A containing residual ammonium sulfate was stored as beads in liquid nitrogen. Enzyme purity was estimated to be approximately 95% by sodium dodecyl sulfate-polyacrylamide gel electrophoresis. Enzyme specific activity was typically 25 nmol min^{-1} mg^{-1} for the wild type and 17−34 nmol min^{-1} mg^{-1} for the mutants. For assays of activity, the enzyme was diluted 1:1000 in 50 mM Tris-HCl (pH 8.0) containing 1 mg/mL bovine serum albumin. For measurements of ligand binding by equilibrium dialysis and for crystallization experiments, the enzyme was dialyzed anaerobically against buffer B [50 mM Tris-HCl (pH 8.0), 0.1 mM EDTA, and 5 mM DTT] prior to being used.

Enzyme Assay. Enzyme activity was assayed by measuring the initial rate of formation of the product glutamate. The standard assay contained 2.5 mM PRPP, 20 mM glutamine, 10 mM $MgCl_2$, 1 mM EGTA, 1 mg/mL bovine serum albumin, 50 mM Tris-HCl (pH 8.0) and approximately 100 ng of enzyme in a total volume of 100 μL. Incubation was at 37 °C for 6 min. The reaction was linear with time for at least 20 min under these conditions of assay (*7*). Reactions were quenched in a boiling water bath for 2 min, and glutamate was determined by the glutamate dehydrogenase method (*2*). The control reaction mixture contained all the components except PRPP.

Inhibition by nucleotides was determined by the standard assay to which varied concentrations of nucleotide were added. Synergistic inhibition was determined by varying the concentration of one nucleotide in the presence of a fixed concentration of a second nucleotide. Relative activity (see Figure 4) refers to the enzyme activity at a given concentation of the *varied* nucleotide relative to that in the absence of the *varied* nucleotide. $I_{0.5}$ refers to the concentration of *varied* nucleotide required to inhibit the enzyme activity by 50%. $I_{0.5}$ values were calculated from plots of relative activity versus *varied* nucleotide concentration.

Nucleotide Binding. Nucleotide binding was determined by equilibrium dialysis (*8*) using chambers of 150 μL that were separated by a 12000−14000 molecular weight dialysis membrane. One chamber contained 0.2 M Tris-HCl (pH 7.5), 20 mM $MgCl_2$, and varied concentrations of a radioactive nucleotide (0−20 mM [2,8-^{3}H]AMP, [8-^{3}H]GMP, [2,8-^{3}H]ADP, or [8-^{14}C]IMP, approximately 0.1 μCi in each case) in a volume of 100 μL. In some experiments, the chambers with radioactive nucleotide also contained a fixed concentration of a second non radioactive nucleotide. The other chamber contained 50 mM Tris-HCl (pH 7.5) and 50−200 μM enzyme, calculated as the subunit concentration, in a volume of 100 μL. Dialysis was carried out for 20 h at room temperature (∼22 °C) in a rotating apparatus. Samples of 80 μL were retrieved from each chamber and were counted for radioactivity. All experiments were performed in an anaerobic glovebox. For all data reported in Table 2, there was less than 10% activity loss at the conclusion of dialysis. Equilibrium binding data were fit to the Hill equation [$Y = C$ [free ligand]^n/[K_d + [free ligand]^n), where Y is the fractional saturation, C is the binding capacity, K_d is the dissociation constant, and n is the Hill coefficient] by nonlinear regression using Ultrafit software (Biosoft, Cambridge, UK).

Crystallization and Structure Solution. Crystals of the ternary enzyme·ADP·GMP complex were grown in glass melting point capillaries by the microbatch method in an anaerobic glovebox. Protein (20 mg/mL) was incubated with 1 mM ADP, 1 mM GMP, and 5 mM $MgCl_2$ and mixed with an equal volume of 24% PEG 8000, 200 mM KCl, 50 mM *N*-(2-hydroxyethyl)piperazine-*N*′-3-propanesulfonic acid (EPPS, pH 7.9), 1 mM ADP, 1 mM GMP, and 5 mM $MgCl_2$. Brown crystals grew to a typical dimension of 0.8 × 0.5 × 0.5 mm over a period of 6−12 weeks. Crystals were cryoprotected for flash freezing by serial transfer, in steps of 5% glycerol, into a cryoprotectant solution of 25% glycerol, 16% PEG 8000, 200 mM KCl, 50 mM EPPS (pH 7.9), 1 mM ADP, 1 mM GMP, and 5 mM $MgCl_2$, in a sitting drop well. The well was sealed with clear plastic tape and removed from the glovebox, and the crystals were rapidly mounted in a small plastic fiber loop and frozen in a nitrogen gas stream at 120 K (*13*). No change in color or diffraction quality of the crystals due to oxygen exposure was observed during this procedure.

Table 1: Data and Refinement Statistics

data	
resolution range (Å)	15.0 - 2.8
no. of observations	195 956 (40.0−2.8 Å)
no. of unique reflections	46 771
completeness (%) (15.0−2.8 Å)	91.0
R_{sym} (%)[a] (40.0−2.8 Å)	8.0
model refinement	
missing residues	76−79, 460−465 for each monomer
total non-hydrogen atoms	14 156
no. of non-protein atoms in model	
Mg^{2+} sites	4
water sites	4
nucleotides	4 GMP plus 4 ADP
data range	15.0−2.8 Å
cutoff [$F/\sigma(F)$]	0.0
R_{work} (%)[b]	21.4
R_{free} (%)[c]	26.4
mean B value (Å^2)	
main chain	30.8
side chain	36.0
rms deviations from ideality	
bonds (Å)	0.016
angles (deg)	2.50
B values (Å^2)	
main chain	2.97
side chain	4.70
noncrystallographic symmetry (Å)	0.09
Ramachandran outliers	none

[a] $R_{sym} = \sum|I_o-\langle I\rangle|/I_o$, where I_o is the observed intensity and $\langle I\rangle$ is the average intensity obtained from multiple observations of symmetry-related reflections. [b] $R_{work} = \sum||F_{obs}| - |F_{calc}||/\sum|F_{obs}|$, where F_{obs} is the observed structure factor and F_{calc} is the structure factor calculated from the final model. The value quoted included all of the reflections, including the ones used for the R_{free} calculation. [c] $R_{free} = \sum||F_{obs}| - |F_{calc}||/\sum|F_{obs}|$ for a random subset of 5% of the total reflections collected.

X-ray diffraction data to a d_{min} of 2.8 Å were collected from a single crystal, flash frozen to 120 K with an Oxford Cryostream, using an R axis II imaging plate system mounted on a Rigaku RU-200 rotating anode (CuKα) operated at 100 mA and 50 kV. Crystals of the 465-residue enzyme grew in the orthorhombic space group $P2_12_12_1$ (a = 160.3 Å, b = 70.4 Å, and c = 182.7 Å), with a homotetramer of approximate $D2$ point symmetry in the asymmetric unit. The data were processed and scaled in the programs DENZO and Scalepack (*14*); data processing statistics are shown in Table 1.

A 2.3 Å model of the AMP-inhibited native *B. subtilis* glutamine PRPP amidotransferase was previously refined using data measured from unfrozen crystals.[3] This structure without the AMP nucleotides was used as an initial model for the ternary enzyme·ADP·GMP complex, which crystallizes isomorphously. All refinement was done with X-PLOR (*15*). Rigid-body refinement of the independent monomers of the tetramer resulted in an R-factor of 36.4% for data between 12.0 and 2.8 Å; inspection of the resulting electron density maps using the program O (*16*) revealed density for the ADP, GMP, and Mg^{2+} bound to the protein. The density clearly distinguished binding sites for ADP and GMP. Subsequent refinement against data from 15.0 to 2.8 Å spacings utilized a test set of 5% of the reflections for R_{free} calculations (*17*) and a bulk solvent mask. Simulated-annealing refinement (*18*) with strict non-crystallographic symmetry constraints yielded an R_{free} of 30.8% and an R_{work} of 26.0%. Conventional positional and grouped B-factor refinement of the tetramer with tightly restrained noncrystallographic symmetry was employed with a Bayesian weighting scheme for structure factors as implemented in the program HEAVY (*19*). A summary of refinement statistics is presented in Table 1.

[3] D. R. Tomchick, J. L. Smith, D. Wolle, and H. Zalkin, Structure of *B. subtilis* glutamine PRPP amidotransferase at 2.3 Å and nucleotide binding studies, Abstract D06, American Crystallographic Association Annual Meeting, Atlanta, GA, 1994.

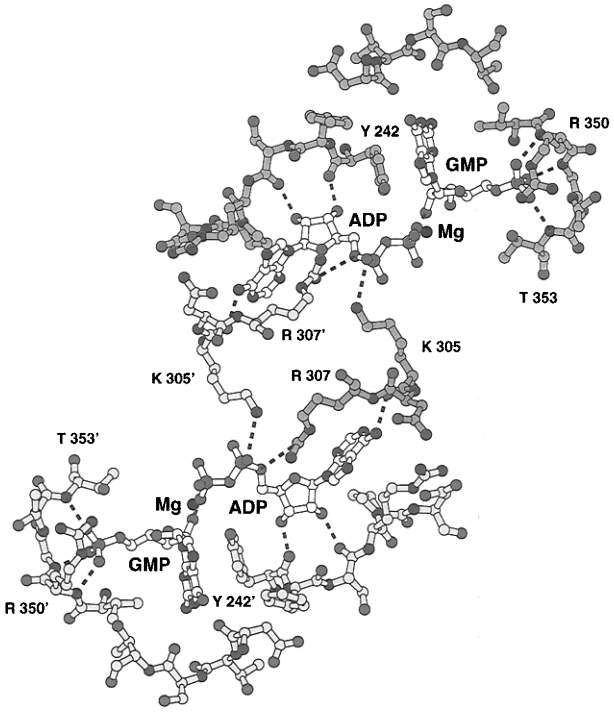

FIGURE 1: View of the 2-fold-related binding sites of glutamine PRPP amidotransferase. GMP is bound in the catalytic PRPP binding site, and ADP is bound in the allosteric site; the Mg^{2+} is drawn as a black sphere. Residues from one monomer are drawn in purple, and residues from the other monomer of the dimer are drawn in yellow; oxygen atoms are red, nitrogen atoms blue, and phosphorus atoms green. Hydrogen bonds are indicated by dashed lines.

RESULTS

Structures of Enzyme Sites with Bound Nucleotides. Earlier work showed that the strongest synergistic pair of nucleotide inhibitors for *B. subtilis* glutamine PRPP amidotransferase is ADP plus GMP (*7*). In order to understand the structural basis for the nucleotide specificity and synergism, the X-ray crystal structure of the ternary enzyme·ADP·GMP complex was determined. Data and refinement statistics are given in Table 1. ADP and GMP bind to sites identified previously as AMP binding sites in the AMP-inhibited enzyme (*6*). Each functional dimer of the amidotransferase contains two catalytic C sites and two allosteric A sites, which are located near the subunit interface (Figure 1). Electron density for the nucleotides clearly demonstrates that GMP binds to the C sites and ADP to the A sites, with no detectable exchange of nucleotides between the two sites (Figure 2).

Residues 341−353 of the C site contain a PRPP-binding sequence motif (*20, 21*) common to type I phosphoribosyltransferases (*22*). This motif forms a hydrophobic β-strand, the PRPP loop itself, which typically contains two acidic

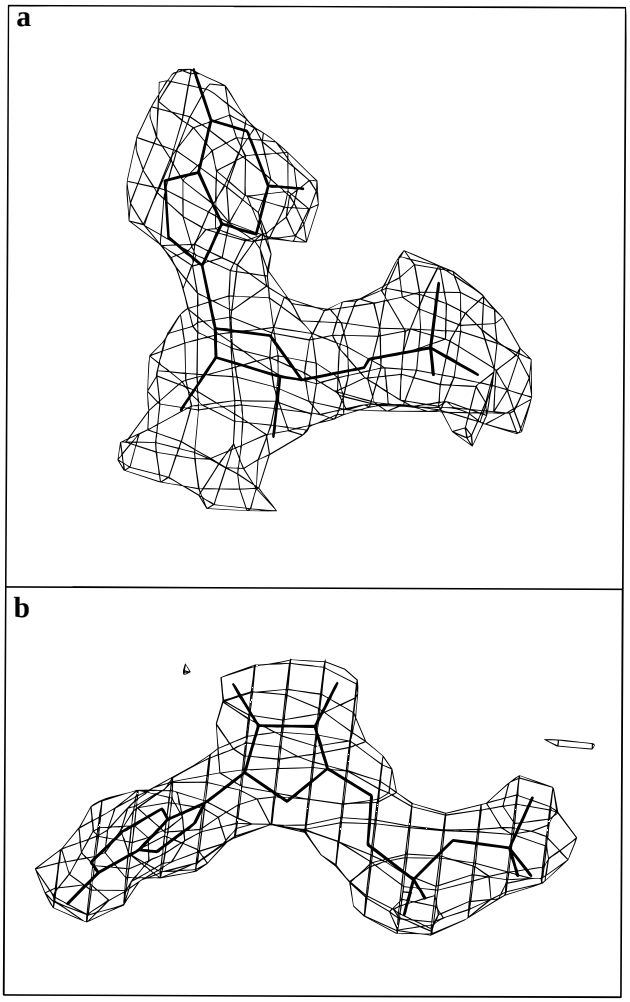

FIGURE 2: Electron density for the bound nucleotides. The map was calculated using $|2F_{obs} - F_{calc}|$ Fourier coefficients, where F_{obs} is the observed structure factor and F_{calc} is the structure factor calculated from the refined model. Electron density is contoured at the rms level of the map. Nucleotides are shown from approximately the same view as the top half of Figure 1. (a) The *syn* GMP bound in the catalytic site. (b) The ADP bound in the allosteric site.

residues (Asp^{345} and Asp^{346}), and the first turn of an α-helix. As in the AMP-inhibited structure, the 5′-phosphate of GMP in this site binds to the NH_2 terminus of the α-helix with hydrogen bonds to backbone amides of the PRPP loop and to the side chain of Arg^{350} (Figure 1). A Mg^{2+} is coordinated to the GMP ribose 2′- and 3′-hydroxyls, to the side chain carboxylate oxygens of Asp^{345} and Asp^{346} in the PRPP loop, to the hydroxyl of Ser^{283}, and to an H_2O molecule (Figure 3). The Mg^{2+} was not detected in the 3.0 Å AMP-inhibited structure (*6*) but was located in the refined 2.3 Å structure in the same coordination environment.[3] In contrast to the adenine base in the AMP-inhibited structure which binds in the usual *anti* conformation, the guanine base of GMP binds in the *syn* conformation (Figure 2a), which is stabilized by a hydrogen bond between the 2-NH_2 group of the guanine and the hydroxyl of Ser^{347} (Figure 3).

Each of the two allosteric A sites at the dimer interface binds an ADP molecule (Figure 1). Binding results from interactions with residues in both subunits. From the primary subunit, there are hydrogen bonds between the backbone carbonyls of Tyr^{242} and Ser^{244} with the 3′- and 2′-hydroxyls, respectively, of the ribose moiety and the ε-NH_2 of Lys^{305}

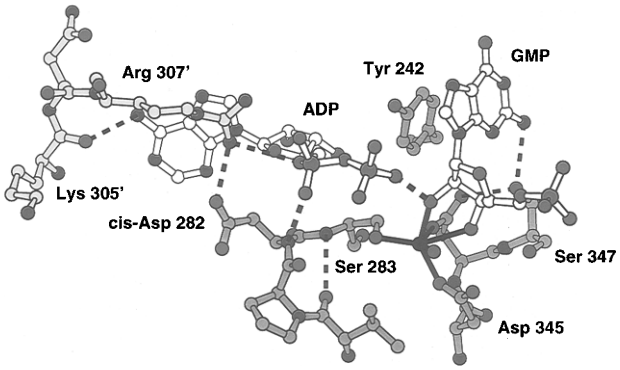

FIGURE 3: View of the nucleotides bound in the catalytic and allosteric sites, emphasizing the GMP-coordinated Mg^{2+} ion and the *cis*-Asp^{282} peptide bond. The coloring scheme is the same as that for Figure 1. Mg^{2+} coordinate bonds are drawn as solid black lines and hydrogen bonds as dashed black lines.

with the ADP α-phosphate (Figure 1). The ε-NH_2 of Lys^{305} is also salt bridged to the carboxylate of Asp^{282} (not shown). Interactions with the secondary subunit occur through the side chain of $Arg^{307'}$, which hydrogen bonds to the α-phosphate of the ADP, and the backbone carbonyl of $Lys^{305'}$. The $Lys^{305'}$ carbonyl hydrogen bonds to the 6-NH_2 group of the adenine base and is responsible for base specificity in the A site which favors purines with a 6-NH_2 group over those with a 6-oxo group. The contribution of amino acid residues from two adjacent subunits to A site nucleotide binding should account, at least in part, for the positive cooperativity of nucleotide inhibition (*6*, *7*).

Inhibitor binding sites in other allosteric enzymes are distant from the active sites and are typically between subunits (*23*). Glutamine PRPP amidotransferase differs from the typical case because the A and C sites are adjacent. Direct contact between the sites occurs via a hydrogen bond between the β-phosphate of ADP in the A site and the ribose 2′-OH of GMP in the C site (Figure 3). This is proposed to be the structural basis for synergistic binding and inhibition by ADP plus GMP.

An unusual *cis* peptide has been observed in a loop adjacent to the C site of all high-resolution glutamine PRPP amidotransferase structures[3] (*4*) and appears to have a functional role in inhibition. Density for this peptide in the ADP·GMP complex is also consistent with a *cis* conformation. An ADP α-phosphate oxygen is hydrogen bonded to the backbone NH of the *cis* peptide in the Pro^{281}-*cis*-Asp^{282}-Ser^{283} turn (Figure 3). Thus, the *cis* conformation seems to be required for inhibition and synergism. The *cis* peptide is also likely to have a role in binding the substrate PRPP or in catalysis because it has also been observed in an analogous position in other type I PRTases (*24*, *25*). A hydrogen bond from NH of the *cis* peptide to the β-phosphate of substrate PRPP would be analogous to the observed hydrogen bond to ADP.

Analysis of Nucleotide Binding. Equilibrium binding measurements, summarized in Table 2, were carried out to quantitate the interactions of nucleotides with the A and C sites. Binding of AMP and ADP extrapolated to 1.57 and 1.83 equiv per subunit, respectively. Thus, AMP and ADP each bound to both the A and C sites. As a consequence of cooperativity, nucleotide binding was analyzed by the Hill equation rather than by the Scatchard equation. Apparent K_d values and Hill coefficients for AMP and ADP are given

Table 2: Nucleotide Binding to the Wild Type Enzyme

nucleotide				
varied	fixed[a] (mM)	capacity[b]	K_d (μM)	Hill coefficient
AMP		1.57 ± 0.27	239 ± 36	3.4 ± 1.8
ADP		1.83 ± 0.26	214 ± 45	1.8 ± 0.65
GMP		ND[c]	ND	ND
ADP	GMP (0.25)	0.82 ± 0.11	10.4 ± 2.7	1.8 ± 0.8
ADP	GMP (1.0)	0.94 ± 0.14	11.0 ± 3.6	1.7 ± 0.9
GMP[d]	ADP (0.5)	0.98 ± 0.10	25 ± 12	2.1 ± 1.0
AMP	GMP (1.0)	1.05 ± 0.21	103 ± 21	2.1 ± 0.80
AMP	ADP (0.25)	0.94 ± 0.16	77 ± 21	2.3 ± 1.2
IMP	ADP (0.25)	0.99 ± 0.22	68 ± 27	1.8 ± 1.0

[a] The millimolar concentration of fixed nucleotide is given in parentheses. [b] Equivalents bound per subunit at saturation ± standard error. [c] ND, not detected. K_d > 0.5 mM. [d] Similar binding in the presence of 0.25 mM ADP (not shown).

in Table 2. Apparent K_d values of 239 and 214 μM for AMP and ADP, respectively, are not true dissociation constants but are equivalent to nucleotide concentrations required for half-saturation of the two sites of each subunit. GMP binding, on the other hand, was too weak to detect, indicative of a K_d greater than approximately 0.5 mM. The Hill coefficient of 3.4 for binding of AMP agrees closely with values of 3.3−3.8 determined from inhibition data (*7*). However, the Hill coefficient for ADP binding of 1.8 is less than the value of 3.8 determined from inhibition data. It is possible that PRPP, present in the assay for inhibition but not in binding measurements, accounts for this difference. Competition between PRPP and adenine nucleotides for the C site is an important factor in the inhibition by AMP and ADP (see the Discussion).

Binding of AMP, ADP, and GMP was also determined in the presence of a fixed concentration of a second nucleotide in order to quantitate synergistic binding. The ADP·GMP pair exhibited the strongest binding synergism. With GMP fixed at either 0.25 or 1.0 mM, approximately 1 equiv of ADP was bound with a K_d of about 10 μM (Table 2, lines 4 and 5). The binding of ADP was thus independent of the fixed concentration of GMP under the conditions used. For the reciprocal case, 1 equiv of GMP was bound to the C site with a K_d of 25 μM in the presence of 0.5 mM ADP (Table 2, line 6). For the GMP·ADP pair, one nucleotide strongly enhanced the binding of the other as can be seen by comparison of these data with the average apparent K_d values for the individual nucleotides shown in lines 2 and 3 of Table 2. This estimate for synergistic binding is greater than 20-fold for the GMP·ADP pair; i.e. $K_{d\ AMP}$ decreased from 214 to 10 μM and $K_{d\ GMP}$ from >500 to 25 μM. The crystal structure of the ternary enzyme·ADP·GMP complex shows that strong synergistic binding of the ADP·GMP pair arises from ADP binding to the A site and GMP binding to the C site and from a direct hydrogen bond between the nucleotides bound in these two sites (Figure 3). Synergistic binding is enhanced by exclusion of each nucleotide from the site to which it does not bind. A base-specific hydrogen bond in the A site likely discriminates against GMP in this site. While ADP is not excluded from the C site, the salt bridge between the GMP 5′-phosphate and Arg^{350} is specific for nucleoside monophosphates and the hydrogen bond between guanine 2-NH_2 and Ser^{347} is specific to *syn* purines with an exocyclic 2-position substituent.

Binding of nucleotide pairs involving AMP is more complex because AMP binds effectively at both the A and C sites. Binding of AMP was determined in the presence of a fixed concentration of either GMP or ADP. Data in Table 2 (lines 7 and 8), indicate binding of approximately 1 equiv of AMP per subunit with similar K_d values of 77 or 103 μM in the presence of ADP or GMP, respectively. With these nucleotide combinations, it is more difficult to assign the site to which AMP bound, because nucleoside monophosphates compete for the C site and adenine nucleotides compete for the A site. For example, when the fixed concentration of ADP was increased from 0.25 to 0.5 mM, the AMP binding stoichiometry was decreased to approximately 0.4 equiv/subunit with a K_d of ∼300 ± 500 μM, indicative of weak binding due to the A site competition (data not shown). It is thus reasonable to infer that AMP binds predominantly to the C site in the presence of ADP and predominantly to the A site in the presence of GMP. Irrespective of the assignment of binding sites, there was only limited synergism for the AMP·GMP and AMP·ADP pairs. The binding affinity for AMP was increased 2−3-fold by GMP or ADP.

To evaluate the importance to C site binding of the Ser^{347} interaction with the amino group at position 2 of the purine ring, binding was determined for IMP, which lacks the 2-amino group, but is otherwise identical to GMP. With ADP bound to the A site, 1 equiv of IMP was bound to the C site with a K_d of 68 μM (Table 2). Thus, the Ser^{347} interaction with the 2-amino group of GMP results in a 3-fold increased binding affinity.

Synergistic Inhibition of the Wild Type Enzyme by Nucleotides. Previous work established the following order for effectiveness of nucleotide inhibitors: AMP > ADP > GDP > GMP (*7*). We determined values for 50% inhibition by AMP, ADP, and GMP (Table 3) that agreed closely with the earlier work. It is important to note that the concentration of ADP required for 50% inhibition is 5 times that for AMP yet apparent binding constants for AMP and ADP shown in Table 2 are similar. We propose, as discussed below in Competition by PRPP and Nucleotide for the C-Site, that this discrepancy results from the different conditions used to measure inhibition and nucleotide binding. The concentration of GMP required for 50% inhibition was 2- and 10-fold higher than that of ADP and AMP, respectively. This is in accord with the weaker binding of GMP relative to the adenine nucleotides, shown in the first three lines of Table 2. The $I_{0.5}$ for IMP was 3-fold higher than that for GMP.

Two methods have been used previously to quantitate synergistic inhibition of glutamine PRPP amidotransferase by nucleotides. In one method, the observed $I_{0.5}$ for an equimolar nucleotide mixture was compared with the value calculated for additive inhibition by each nucleotide of the pair (*2*, *7*). A second approach has been to compare the observed inhibition by arbitrary concentrations of nucleotide pairs with that calculated for additive inhibition (*8*). For this work, we have developed a more systematic method for quantitating synergism by nucleotide pairs. For a given nucleotide pair, ADP·GMP for example, the $I_{0.5}$ for one member was determined in the presence of a fixed concentration of the other. Enzyme inhibition by ADP determined in the presence of different fixed concentrations of GMP is shown in Figure 4. An $I_{0.5\ ADP}$ of 0.24 mM was obtained at a fixed GMP concentration of 0.25 mM (Table 3). Thus, binding of GMP to the C site reduced the $I_{0.5\ ADP}$ from 4.7 mM (no GMP) to 0.24 mM, a 20-fold synergism. However,

Table 3: Summary for Inhibition of Wild Type and Mutant Enzymes by Nucleotides

nucleotide		wild type		S283A		K305Q		R307Q		S347A	
varied	fixed[a]	$I_{0.5}$ (mM)	synergism[b]	$I_{0.5}$ (mM)	synergism	$I_{0.5}$ (mM)	synergism	$I_{0.5}$ (mM)	synergism	$I_{0.5}$ (mM)	synergism
AMP		0.9		6.1		2.5		2.6		1.5	
ADP		4.7		24		31		28		8.1	
GMP		9.4		6.6		50		50		14	
IMP		26								41	
ADP	GMP (0.25)	0.24	20								
ADP	GMP (0.50)	0.16	29	4.8	5.0	12	2.6	2.4	12		
ADP	GMP (1.0)	0.08	59							0.22[c]	37
ADP	GMP (2.0)	0.04	118								
ADP	GMP (4.0)	0.025	188								
ADP	GMP (5.0)					0.32	97	0.18	156		
GMP	ADP (0.5)	0.15	63	2.0	3.3	6.0	8.3	3.3	15	0.44[c]	33
GMP	ADP (2.5)			1.7	3.9	1.3	38	0.76	66		
IMP	ADP (0.5)	0.93	28							1.6[c]	26
AMP	ADP (0.5)	0.64	1.4							0.65[c]	2.3
AMP	GMP (1.0)	0.94	1.0							1.8[c]	0.8
GMP	AMP (0.1)	9.9	0.95								
ADP	AMP (0.1)	2.5	1.9								

[a] The millimolar fixed nucleotide concentration is in parentheses. [b] Decreased $I_{0.5}$ due to a second nucleotide. The concentration of the second nucleotide was approximately 0.1 of its individual $I_{0.5}$. [c] Fixed nucleotide concentrations were 1.4 mM GMP and 0.8 mM ADP rather than the values shown in column 2.

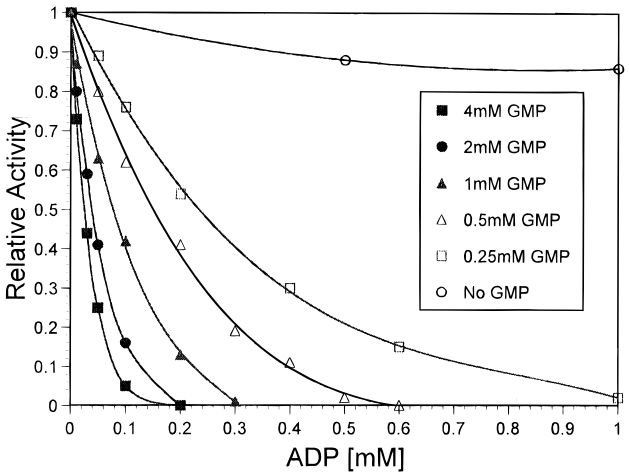

FIGURE 4: Effect of different fixed concentrations of GMP on the inhibition by ADP. At each of six fixed GMP concentrations, the enzyme activity observed in the absence of ADP was assigned a relative activity of 1.0 and the inhibition by ADP was determined.

as shown in Figure 4 and Table 3, the inhibition by ADP and therefore the synergism are dependent upon the concentration of the fixed nucleotide. $I_{0.5\ ADP}$ varied 10-fold depending upon the fixed GMP concentration. This is due to competition between PRPP and GMP for the C site. The competitive relationship between PRPP saturation and nucleotide inhibition has been described for the *B. subtilis* enzyme (*7*). To standardize comparisons of different nucleotide pairs with wild type and standardize comparisons with mutant enzymes, synergism was calculated using a fixed nucleotide concentration set to approximately 0.1 of its $I_{0.5}$ when assayed individually. Accordingly, at a fixed concentration of 1.0 mM GMP, the $I_{0.5\ ADP}$ was 0.08 mM with 59-fold synergism (0.08 versus 4.7 mM). For the reciprocal case, titration of GMP at a fixed concentration of 0.5 mM ADP (approximately 0.1 of the $I_{0.5\ ADP}$ of 4.7) gave an $I_{0.5\ GMP}$ of 0.15 mM and 63-fold synergism (0.15 versus 9.4 mM). The average value for synergism of the ADP·GMP pair is therefore 61. For the ADP·IMP pair, synergism was 28. By contrast, the average synergism for the AMP·ADP pair was 1.7, and there was no synergism for the AMP·GMP pair.

Mutations of A and C Site Residues That Interact with Nucleotides. We have replaced four residues that interact with nucleotides bound in the A and C sites and have examined the effects of these mutations on inhibition and synergism. Summarized data are given in Table 3 for inhibition of mutant enzymes S283A, K305Q, R307Q, and S347A by individual nucleotides and nucleotide mixtures.

The Ser^{283} hydroxyl is a ligand to the octahedrally coordinated Mg^{2+} in the C site (Figure 3). The other five ligands are the carboxylates of Asp^{345} and Asp^{346}, the ribose 2′- and 3′-hydroxyls of the C site nucleotide, and a water molecule. Furthermore, the Pro^{281}-*cis*-Asp^{282}-Ser^{283} turn occupies a central location between the A and C sites, and mutations here might be expected to impact nucleotide binding in either site. $I_{0.5}$ concentrations for AMP and ADP were increased 5−7-fold in the S283A mutant relative to that of the wild type enzyme, whereas the inhibition by GMP was similar for the mutant and wild type. These results suggest that S283A has a greater impact on nucleotide binding to the A site than to the C site because AMP and ADP bind to both nucleotide sites, whereas high-affinity GMP binding is predominantly to the C site. Inhibition by an ADP·GMP mixture demonstrated substantially reduced synergistic inhibition by S283A. With an ADP·GMP mixture, a 30-fold higher concentration of ADP and a 13-fold higher concentration of GMP were required for 50% inhibition compared to that of wild type. Synergism for the ADP·GMP pair was 4.5-fold, the average calculated from $I_{0.5}$ concentrations for ADP (synergism of 5.0) and GMP (synergism of 3.9), compared to 61-fold for wild type. Loss of synergism thus could account for the defective inhibition by the ADP·GMP mixture even though the inhibition by GMP alone was not perturbed. The impact of S283A on the A site is explained most directly by effects on the Pro^{281}-*cis*-Asp^{282}-Ser^{283} turn, which binds the phosphate moiety of the A site nucleotide (Figure 3). The Ser^{283} hydroxyl Mg^{2+} ligand, lost in the mutation, is likely replaced by water and is expected to cause subtle changes in the conformation of the Pro^{281}-*cis*-Asp^{282}-Ser^{283} turn. Such changes could perturb A site nucleotide binding directly or indirectly through salt

bridges between the A site nucleotide α-phosphate and the side chain of Lys^{305} and Arg$^{307'}$ (Figure 1).

Lys^{305} and Arg^{307} interact with nucleotide in the A site. In addition to the salt bridges just described, the backbone oxygen of Lys$^{305'}$ forms a base-specific hydrogen bond with adenine N_6. Arg$^{307'}$ N_η interacts with the α-phosphate and also with the carboxylate of *cis*-Asp^{282}. The latter interaction links Arg$^{307'}$ with Ser^{283} (Figure 3). The two A site mutations, K305Q and R307Q, had similar effects. $I_{0.5}$ concentrations for inhibition by a single nucleotide were increased 3−6-fold compared to that of the wild type. This effect was amplified for inhibition by the ADP·GMP nucleotide pair, for which $I_{0.5}$ values were increased 15−75-fold. Synergism for the ADP·GMP pair was approximately 111 for R307Q (average of 156 and 66) and 68 (average of 97 and 38) for Lys305Q, variations of less than 2-fold from the value of the wild type. Although these residues interact with the A site nucleotide, the perturbations were comparable for inhibition by ADP at the A site and by GMP at the C site. As a consequence of synergism, decreased affinity of ADP for the mutant A site perturbs inhibition by GMP at the C site.

The side chain of Ser^{347} makes a key, base-specific interaction with the guanine 2-amino group of GMP in the C site. This H bond stabilizes the *syn* conformation of GMP in the C site and is expected to contribute to the C site preference for GMP. IMP lacks the 2-amino substituent but is otherwise identical to GMP. For the wild type enzyme, $I_{0.5}$ was 6-fold higher for IMP than for GMP, determined in each case with ADP bound to the A site, and synergism was 2-fold lower, thus supporting the contribution of Ser^{347} to GMP binding in the C site. In the S347A mutant, there were comparable changes for inhibition by GMP and IMP at the C site. $I_{0.5\ GMP}$ and $I_{0.5\ IMP}$ increased 3-fold and 2-fold, respectively, compared to that of the wild type. Synergism was similar for GMP·ADP in S347A, for IMP·ADP in S347A, and for IMP·ADP in the wild type, with values of 26−33 which were about half of that obtained with GMP·ADP in the wild type enzyme. Thus, GMP and IMP exhibit similar synergism with ADP in the absence of the guanine-specific hydrogen bond to Ser^{347}. The S347A mutation does not, however, equalize the inhibition for GMP and IMP; GMP is still a better inhibitor. In the absence of the hydrogen bond to Ser^{347}, GMP may bind in the *anti* conformation, which might afford other hydrogen bonding opportunities for the 2-amino group. Interpretation of the S347A data is also complicated by a second hydrogen bond from the side chain of Ser^{347} to that of Asp^{346} (Figure 3). Subtle structural changes in the PRPP binding loop may result from elimination of this hydrogen bond in S347A. This is supported by measurements of $K_{m\ PRPP}$. Values of $K_{m\ PRPP}$ of 75−81 μM were obtained for the wild type, S283A, K305Q, and R307Q enzymes, but a $K_{m\ PRPP}$ of 182 μM was obtained for the S347A enzyme (data not shown).

DISCUSSION

The interaction of ligands with two sites, nucleotide to an allosteric A site and nucleotide and PRPP competing for a catalytic C site, determines the extent of inhibition of glutamine PRPP amidotransferase. The data reported here define the structural features that dictate the binding of nucleotides to these sites and the resulting inhibition. Purine nucleoside mono- and diphosphates, AMP, GMP, and ADP, each bind to the A and C sites to exert inhibition. There are five principal conclusions from our analyses. (i) Each of the sites has limited specificity, favoring certain nucleotides over others. (ii) Synergistic inhibition by the ADP·GMP nucleotide pair results from synergistic binding. (iii) Synergistic binding results from an interaction between ADP in the A site and GMP in the C site. (iv) Competition between PRPP and nucleotide for the C site amplifies synergism and explains the more effective inhibition of AMP compared to that of ADP. (v) Inhibition requires nucleotide binding to both sites. These conclusions are discussed below.

Specificity of Nucleotide Sites. The x-ray structural model of the nucleotide A and C sites for the ternary ADP·GMP·enzyme complex shown in Figures 1 and 3, together with the structure of the AMP complex (*6*), explains the adenine nucleotide specificity for the A site and GMP specificity for the C site. The specificities result mainly from base-specific H bonds between the Lys$^{305'}$ backbone oxygen and the adenine 6-amino group in the A site and between the Ser^{347} hydroxyl and the guanine 2-amino group in the C site. The adenine-specific hydrogen bond in the A site discriminates against other nucleotides in this site, which can accommodate only the *anti* conformation of the nucleotide. The C site is more spacious, and the crystal structures show that AMP binds in the *anti* conformation and GMP in the *syn*. The Ser^{347} hydrogen bond with the GMP 2-amino group provides a modest 3-fold-increased binding affinity for GMP to the C site relative to those of IMP and AMP, which lack the 2-amino group (Table 2).

There is a second specificity determinant. Nucleoside mono- and diphosphates should have equal access to the A site, but nucleoside monophosphates are favored in the C site. This is because there are no barriers to monophosphates or diphosphates in the A site, whereas there is a steric clash for a nucleoside diphosphate in the C site. Without rearrangement of residues in the PRPP loop, there is insufficient space for the β-phosphate of a nucleoside diphosphate. Nevertheless, ADP was bound to both sites with a value for half-saturation that is similar to that for AMP (Table 2). Thus, rearrangements of the PRPP loop can accommodate a nucleoside diphosphate in the C site.

Finally, a Mg^{2+} is required for nucleotide binding to both the C and A sites. Meyer and Switzer (*7*) demonstrated distinct metal ion requirements for inhibition and for catalysis. The Mg^{2+} allows the C site nucleotide to bind to the protein via its coordination to the ribose 2′-OH and 3′-OH and the Asp^{345} and Asp^{346} carboxylates and helps to neutralize the relatively high local negative charge in the vicinity of these aspartate residues. The importance of this metal ion for inhibition is emphasized by the observation that binding of nucleotide to either site is abolished in the absence of Mg^{2+}, as determined by equilibrium dialysis (data not shown).

Synergistic Nucleotide Binding. Synergistic binding of the ADP·GMP pair accounts for the observed synergistic inhibition. In the presence of GMP the K_d for ADP was decreased 20-fold from approximately 214 to 11 μM. It is necessary, however, to recognize that binding of ADP to the free enzyme is complex, involving cooperative binding to two A sites and two C sites per dimer. Thus, the K_d of 214 μM, in this instance, is an operational assessment of half-saturation of the two sites. In the presence of GMP, the K_d

for ADP is more simply defined as half-saturation of the A site. In the reciprocal experiment, the K_d for GMP was decreased from an unmeasurable concentration to 25 μM in the presence of ADP. Assuming a synergism of 20-fold, we estimate a K_d of GMP for the free enzyme of approximately 500 μM.

The structural model for the enzyme·ADP·GMP complex explains the physical basis for synergism. There are three key points. First, ADP and GMP are each bound to their preferred sites. For this nucleotide pair, there is minimal competition between nucleotides for each site. Competition between nucleotides for a site minimizes the opportunity for a productive nucleotide−nucleotide interaction. Even though AMP and IMP have similar affinities for binding to the C site (Table 2), competition of AMP, but not IMP, with ADP for the A site explains the difference in synergism between IMP·ADP and AMP·ADP (Table 3). Second, the nucleotide−nucleotide interaction is not possible with nucleoside monophosphates in both sites. Third, the octahedrally coordinated Mg^{2+} is important not only for inhibition by nucleotides but also for synergism. This requirement is explained by the structural model in which the ribose 2′- and 3′-hydroxyls of the C site nucleotide are ligands to the Mg^{2+} (Figure 3). The large reduction in synergism in the S283A mutant provides evidence that the Ser^{283} β-hydroxyl ligand to the Mg^{2+} is required for synergism. This interaction positions the unusual Pro^{281}-*cis*-Asp^{282}-Ser^{283} turn, which is part of both the A and C sites. In the absence of Mg^{2+} coordination in the S283A mutant, the Pro^{281}-*cis*-Asp^{282}-Ser^{283} turn may have a different conformation, repositioning the A and C sites with respect to one another. A very small structural change could effectively eliminate the interaction between the C site ribose 2′-OH and the A site ADP β-phosphate, and thus decrease synergism. Without this nucleotide−nucleotide interaction, there is minimal synergistic binding for AMP·GMP. AMP is the most potent single nucleotide inhibitor. However, as a consequence of synergism, an ADP/GMP mixture inhibits more strongly than AMP.

Synergistic Inhibition. Synergistic inhibition of glutamine PRPP amidotransferase by particular nucleotide pairs is a regulatory mechanism that enables cells to monitor and adjust the pools of adenine and guanine nucleotides, the end products of *de novo* biosynthesis. ADP and GMP are the strongest synergistic pair for the *B. subtilis* enzyme (Table 3 and ref 7). There are two key features of synergism. First, the inhibition by each nucleotide is amplified. AMP is the most potent single nucleotide inhibitor. However, as a consequence of synergism, an ADP/GMP mixture inhibits more strongly than AMP. Second, inhibition by one nucleotide is dependent upon the fixed concentration of the partner. As shown in Table 3, values for 50% inhibition by ADP were dependent upon the fixed GMP concentration. This is because of competition between GMP and PRPP for the C site. In the absence of PRPP, the C site was saturated by 0.25 mM GMP with ADP bound to the A site (Table 2). However, 10-fold or higher concentrations of GMP were required for C site saturation when PRPP was present (Table 3). It is obviously technically impossible to determine the concentration required for 50% inhibition by one nucleotide in the presence of a saturating concentration of a second. For this reason, synergism was defined as the increased inhibition by one nucleotide at an arbitrary fixed concentration of the partner. The ADP·GMP synergism varies in parallel with the concentration of either nucleotide, thus further amplifying the regulatory response. The synergism for ADP·IMP was about half that of ADP·GMP, and there was little or no synergism for ADP·AMP and GMP·AMP. Although not studied here, two other nucleotide pairs, ADP·GDP and GDP·GMP, were reported to give synergistic inhibition (*7*).

Of the mutations that perturbed nucleotide binding, synergism was affected most by the Ser^{283} replacement and little, if at all, by replacements of Lys^{305} and Arg^{307}. ADP/GMP synergism was reduced only minimally from 60-fold in the wild type to 35-fold in the S347A mutant. Two results stand out. In assays of A and C site function using the ADP·GMP pair, inhibition at both sites was comparably perturbed in each of the mutants. That is, in no case did a mutation selectively disable one site. Second, the inhibition at the A and C sites by the nucleotide mixture was decreased more than inhibition by individual nucleotides. Thus, site−site interaction was more sensitive to mutational disruption than an individual site. In this context, the Pro^{281}-*cis*-Asp^{282}-Ser^{283} turn could be called the "synergistic turn", emphasizing its key role in synergism.

Competition between PRPP and Nucleotide for the C Site. There are two important consequences of C site competition between PRPP and nucleotide. First, as explained above, in the presence of PRPP, inhibition by ADP at the A site is dependent on the nucleotide versus PRPP competition for the C site. This amplifies synergism, as shown by comparing the 20-fold synergistic binding of ADP (+GMP) (Table 2), determined in the absence of PRPP, with the nearly 200-fold synergism for inhibition by ADP (+GMP) (Table 3), determined in the presence of PRPP. Second, competition between nucleotide and PRPP can explain the more effective inhibition by AMP compared with that by ADP. Given the fact that the apparent K_d values for ADP and AMP are identical (Table 2), it is surprising that 5-fold higher concentrations of ADP, relative to those of AMP, were required for 50% inhibition (Table 3). A plausible explanation is that PRPP competes more effectively with ADP for the C site due to steric clash of the ADP β-phosphate with residues of the PRPP loop. Furthermore, binding of PRPP to the C site may exclude binding of ADP but not AMP to the A site due to overlap of binding sites for the β-phosphate of PRPP and the β-phosphate of ADP in the A site.

Inhibition Requires Nucleotide Binding to both A and C Sites. Two lines of evidence support the conclusion that binding of nucleotides to both sites is necessary for inhibition. First, by direct measurement the affinity of the C site for GMP was determined to be 3-fold higher than that, for AMP, in each case with ADP bound to the A site. The fact that half-saturation of the A plus C sites required 240 μM AMP whereas GMP binding was too weak to detect indicates that weak affinity of GMP for the A site precluded detection of C site binding. Second, A site mutations K305Q and R307Q had as much of an effect on inhibition by GMP as on inhibition by ADP, and a C site mutation, S347A, likewise had a comparable effect on inhibition by these two nucleotides. If nucleotide binding to one site were sufficient for inhibition, A site mutations should preferentially disable ADP binding and inhibition, and the C site mutation should preferentially perturb GMP binding and inhibition. The S283A mutant is closest to having selective loss of inhibition

by one nucleotide. In this mutant, inhibition by GMP was similar to that of the wild type whereas there was 5−7-fold-decreased inhibition by AMP or by ADP. However, even in this mutant, synergistic inhibition at both the A and C sites was decreased for the ADP·GMP pair. In contrast to the *E. coli* enzyme where an A site mutation selectively decreased binding to the A site and inhibition (*8*), mutations in either of the nucleotide sites of the *B. subtilis* glutamine PRPP amidotransferase perturbed the function at both sites.

The synergistic binding of adenine and guanine nucleotides to the A and C sites has important physiological consequences. A single pathway for *de novo* purine nucleotide synthesis results in the production of adenine and guanine nucleotides. Whereas uptake of either base or nucleoside can elevate the pool of the corresponding nucleotide (*26*) and repress gene transcription by different mechanisms (*27*), glutamine PRPP amidotransferase has been designed to regulate biosynthesis by sensing the availability of both nucleotides. Feedback inhibition by one nucleotide is inefficient, and *de novo* synthesis should continue until both nucleotides are in excess. Enzyme binding sites have been optimized to monitor the availability of both nucleotides and to integrate this information with biosynthetic capacity as reflected by the PRPP pool in order to amplify the synergistic regulatory response.

REFERENCES

1. Zalkin, H., and Smith, J. L. (1998) *Adv. Enzymol. Relat. Areas Mol. Biol.* (in press).
2. Messenger, L. J., and Zalkin, H. (1979) *J. Biol. Chem. 254*, 3382−3392.
3. Wong, J. Y., Bernlohr, D. A., Turnbough, C. L., and Switzer, R. L. (1981) *Biochemistry 20*, 5669−5674.
4. Muchmore, C. R. A., Krahn, J. M., Kim, J. H., Zalkin, H., and Smith, J. L. (1997) *Protein Sci.* (in press).
5. Krahn, J. M., Kim, J. H., Parry, R. J., Zalkin, H., and Smith, J. L. (1997) *Biochemistry* (in press).
6. Smith, J. L., Zaluzec, E. J., Wery, J.-P., Niu, L., Switzer, R. L., Zalkin, H., and Satow, Y. (1994) *Science 264*, 1427−1433.
7. Meyer, E., and Switzer, R. L. (1979) *J. Biol. Chem. 254*, 5397−5402.
8. Zhou, G., Smith, J. L., and Zalkin, H. (1994) *J. Biol. Chem. 269*, 6784−6789.
9. Makaroff, C. A., Zalkin, H., Switzer, R. L., and Vollmer, S. J. (1983) *J. Biol. Chem. 258*, 10586−10593.
10. Kunkel, T. A., Roberts, J. D., and Zakour, R. A. (1987) *Methods Enzymol. 154*, 367−382.
11. Tso, J. Y., Zalkin, H., vanCleemput, M., Yanofsky, C., and Smith, J. M. (1982) *J. Biol. Chem. 257*, 3525−3531.
12. Makaroff, C. A., and Zalkin, H. (1986) *J. Biol. Chem. 261*, 11416−11423.
13. Teng, T. Y. (1990) *J. Appl. Crystallogr. 23*, 387−391.
14. Otwinowski, Z. (1993) in *Data Collection and Processing* (Sawyer, N. I. L., and Bailey, S., Eds.) pp 56−62, Science and Engineering Research Council Daresbury Laboratory, Daresbury, UK.
15. Brunger, A. T. (1992a) *XPLOR Version 3.1, A System for X-ray Crystallography and NMR*, Yale University Press, New Haven, CT.
16. Jones, T. A., Zou, J. Y., Cowan, S. W., and Kjeldgaard, M. (1991) *Acta Crystallogr. A 47*, 110−119.
17. Brunger, A. T. (1992b) *Nature 355*, 372−475.
18. Brunger, A. T., Krukowski, A., and Erickson, J. W. (1990) *Acta Crystallogr. A 46*, 585−593.
19. Terwiller, T. C., and Berendzen, J. (1995) *Acta Crystallogr. D 51*, 609−618.
20. Hershey, H. V., and Taylor, M. (1986) *Gene 43*, 287−293.
21. Hove-Jensen, B., Harlow, K. W., King, C. J., and Switzer, R. L. (1986) *J. Biol. Chem. 261*, 6765−6771.
22. Eads, J., Ozturk, D., Wexler, T. B., Grubmeyer, C., and Sacchettini, J. C. (1997) *Structure 5*, 47−58.
23. Perutz, M. (1989) *Mechanisms of Cooperativity and allosteric Regulation in Proteins*, Cambridge University Press, Cambridge, UK.
24. Henriksen, A., Aghajari, N., Jensen, K. F., and Gahede, M. (1996) *Biochemistry 35*, 3803−3809.
25. Somoza, J. R., Chin, M. S., Focia, P. J., Wang, C. C., and Fletterick, R. J. (1996) *Biochemistry 35*, 7032−7040.
26. Saxild, H. H., and Nygaard, P. (1991) *J. Gen. Microbiol. 137*, 2387−2394.
27. Ebbole, D. J., and Zalkin, H. (1987) *J. Biol. Chem. 262*, 8274−8287.

BI9711893